

Article

Selection of Bias Correction Methods to Assess the Impact of Climate Change on Flood Frequency Curves

Enrique Soriano * , Luis Mediero  and Carlos Garijo 

Department of Civil Engineering: Hydraulic, Energy and Environment, Universidad Politécnica de Madrid, 3, 28040 Madrid, Spain; luis.mediero@upm.es (L.M.); c.garijo@upm.es (C.G.)

* Correspondence: e.soriano@upm.es; Tel.: +34-910674372

Received: 5 September 2019; Accepted: 21 October 2019; Published: 29 October 2019



Abstract: Climate projections provided by EURO-CORDEX predict changes in annual maximum series of daily rainfall in the future in some areas of Spain because of climate change. Precipitation and temperature projections supplied by climate models do not usually fit exactly the statistical properties of the observed time series in the control period. Bias correction methods are used to reduce such errors. This paper seeks to find the most adequate bias correction techniques for temperature and precipitation projections that minimizes the errors between observations and climate model simulations in the control period. Errors in flood quantiles are considered to identify the best bias correction techniques, as flood quantiles are used for hydraulic infrastructure design and safety assessment. In addition, this study aims to understand how the expected changes in precipitation extremes and temperature will affect the catchment response in flood events in the future. Hydrological modelling is required to characterize rainfall-runoff processes adequately in a changing climate, in order to estimate flood changes expected in the future. Four catchments located in the central-western part of Spain have been selected as case studies. The HBV hydrological model has been calibrated in the four catchments by using the observed precipitation, temperature and streamflow data available on a daily scale. Rainfall has been identified as the most significant input to the model, in terms of its influence on flood response. The quantile mapping polynomial correction has been found to be the best bias correction method for precipitation. A general reduction in flood quantiles is expected in the future, smoothing the increases identified in precipitation quantiles by the reduction of soil moisture content in catchments, due to the expected increase in temperature and decrease in mean annual precipitations.

Keywords: bias correction; quantile mapping; climate change; floods; CORDEX

1. Introduction

Climate change projections predict reductions in the availability of water resources, as well as changes in the frequency and severity of extreme hydrological events [1]. Consequently, climate change will affect floods, which are the natural hazard that generates the largest damages in Europe [2]. The impact of climate change on the hydrological cycle can be assessed by using both climatic and hydrological models. Several studies and models have been developed. However, most of such studies are focused on either monthly or annual scales [3]. Only a few studies have studied the impact of climate change on floods [4].

Global climate models (GCMs) are large-scale models that simulate the behavior of atmospheric circulation patterns with a gross resolution of approximately 100–250 km. Consequently, downscaling techniques are required to obtain results at finer resolutions of around 25–50 km [5]. Regional climate models (RCM) are the most usual downscaling technique.

Outputs of climate models in the control period do not usually fit exactly the statistical properties of observations at gauging stations in the same period. Bias errors between climate models and observations can be caused by an imperfect conceptualization, discretization and spatial averaging within grid cells. For example, bias errors usually occur on very wet days with small rainfall intensities or extreme temperatures. Biases in the outputs of RCMs can lead to unrealistic hydrological simulations of river streamflows [6,7]. Bias correction is the process of scaling climate model outputs to account for their systematic errors, in order to improve their fitting to observations. Several bias correction methods exist [8]. Linear scaling corrects projections based on monthly errors [9]. Further bias correction focusing on days with precipitation can be obtained by the local intensity scaling approach [10]. The power transformation approach can correct biases in the mean and variance [11]. Quantile mapping can correct the distribution function of a given variable usually utilizing a Gaussian or gamma distribution function to improve its fitting to observations [12]. Most of such approaches focus on correcting precipitation and time series supplied by climate projections to improve their fitting to observations, regardless of the extreme value behavior. Quantile mapping tries to improve the fitting of higher values of precipitation through a gamma distribution function. However, bias correction techniques do not consider the fitting to frequency curves. Some studies consider the influence of bias correction on flow frequency curves. However, the best methodology is selected based on the improvement in the complete time series instead of focusing on the extreme values that are included in the frequency curve [13].

In Spain, there are two sources of climate projections: AEMET ('Agencia Estatal de Meteorología', in Spanish) [14,15] and EURO-CORDEX [16]. AEMET uses atmospheric data obtained from the National Center for Atmospheric Research (NCAR) reanalysis. Precipitation and temperature data are supplied with a high-resolution grid of 203 points. This grid was obtained from the data bank of the National Institute of Meteorology [17].

EURO-CORDEX is the European branch of the international CORDEX initiative, which is a program sponsored by the World Climate Research Program (WRC), seeking to organize an internationally coordinated framework to produce improved regional climate change projections for worldwide regions. The CORDEX results will serve as input for climate change impact and adaptation studies within the timeline of the Fifth Assessment Report (AR5) of the Intergovernmental Panel on Climate Change (IPCC).

AEMET precipitation projections do not characterize adequately extreme events at the Spanish national scale [18]. However, EURO-CORDEX precipitation projections adequately characterize the statistical properties of annual maximum precipitation series in Spain [19]. Consequently, climate projections supplied by the EURO-CORDEX initiative are used in this study. Such climate projections point out that precipitation quantiles will increase in some parts of Spain [20].

Impacts of climate change on floods should be assessed to update flood risk management plans, considering how they are expected to vary in the future. In addition, peak flow quantiles are useful for infrastructure design and safety assessment. This paper is focused on assessing how peak flow quantiles are expected to change in the future. Most of bias correction techniques do not consider their impact on flood frequency curves that are obtained from corrected precipitation and temperature projections [21]. Consequently, a methodology to identify the best bias correction method in precipitation and temperature projections to improve the fitting of flood frequency curves in the control period to observations is proposed. In addition, expected flood frequency curves in the future under climate change conditions are provided [22].

Bias corrected temperature and precipitation projections are used as input data of the continuous hydrological Hydrologiska Byråns Vattenbalansavdelning model (HBV), which is calibrated with the methodology proposed previously. Four catchments in northwestern Spain are selected as case studies.

This paper is organized as follows. First, the case studies and data sources are presented. Second, the tools and methodology used in the study are described. Third, the results of bias correction in

temperature and precipitation time series are discussed. Fourth, results about flood frequency curves expected in the future are presented. Finally, conclusions are provided.

2. Data and Methodology

The methodology consists of the following steps: (i) Calibration of the HBV model to adequately characterize rainfall-runoff processes in a changing climate; (ii) selection of the best bias correction method for precipitation and temperature projections, and (iii) assessment of the expected changes in flood quantiles in the future driven by climate change.

2.1. Study Area and Data

Four catchments in the Douro river basin in the northwestern part of Spain have been selected as case studies (Figure 1 and Table 1). A dam is located at the outlet of each catchment. Consequently, inflow discharges in reservoirs were estimated from observations of mean daily reservoir water levels and dam releases, which were supplied by the Centre for Hydrographic studies of CEDEX.

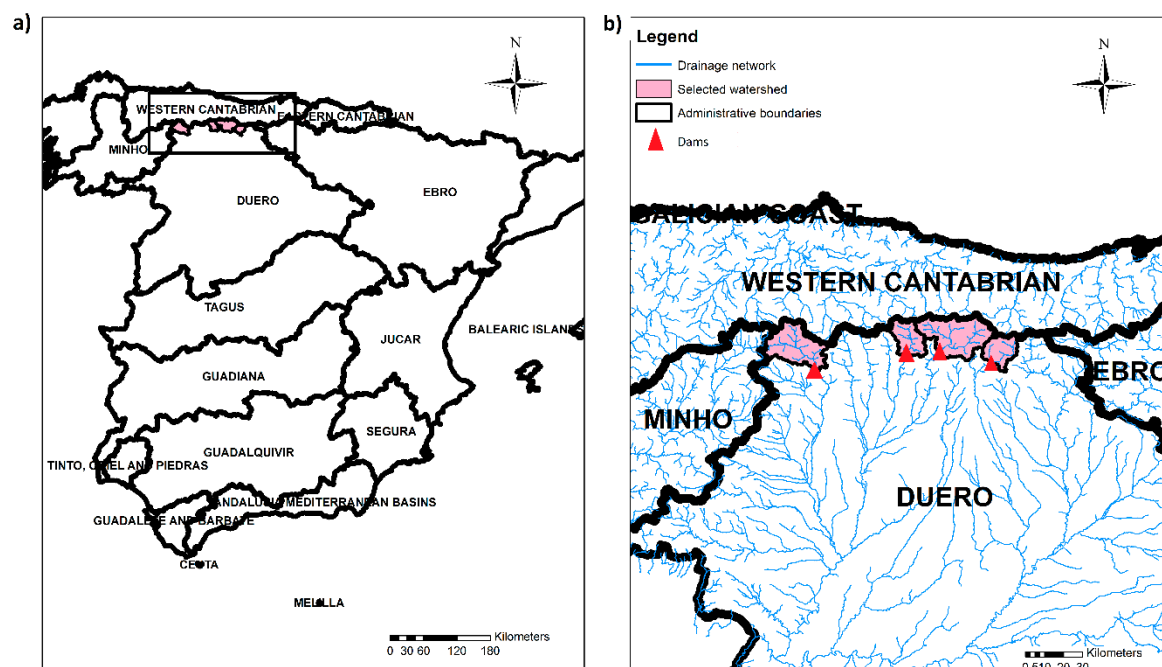


Figure 1. (a) Location of the four case studies in Spain; (b) catchments of the four case studies.

Table 1. Catchment characteristics.

Catchment Descriptors	Barrios de Luna	Camporredondo	Porma	Riaño
Area (km ²)	491.86	230	249.64	593
River Length (km)	36.23	28.43	23.12	36.16
Maximum altitude (m)	2409.58	2532.23	2160.91	2492.52
Minimum altitude (m)	1084.11	1285	1091.99	1081.5

Observations of daily rainfall at 42 rain-gauging stations and temperature at 22 thermometric stations were supplied by the AEMET. Gaps in time series were filled by using observations at nearby gauging stations, by using the inverse distance weighting (IDW) method with squared distances.

Climate change projections provided by 12 regional climate models of the EURO-CORDEX programme have been used (Table 2). Such projections are composed of daily rainfall and temperature time series in a grid with cells of 0.11°. The same control period (1971–2004, hydrological years) and

future period under climate change (2011–2094, hydrological years) have been considered for all the climate models. Two representative concentration pathways (RCP) were considered: RCP 4.5 and 8.5.

Table 2. EURO-CORDEX climate models used in the study.

Acronym	CGM	RCM
ICH-CCL	ICHEC-EC-EARTH	CCLM4-8-17
MPI-CCL	MPI-ESM-LR	CCLM4-8-17
MOH-RAC	MOHC-HadGEM2-ES	RACMO22E
CNR-CCL	CNRM-CMS	CCLM4-8-17
ICH-RAC	ICHEC-EC-EARTH	RACMO22E
MOH-CCL	MOHC-HadGEM2-ES	CCLM4-8-17
IPS-WRF	IPSL-CMSA-MR	WRF331F
IPS-RCA	IPSL-CM5A-MR	RCA4
MOH-RCA	MOHC-HadGEM2-ES	RCA4
ICH-RCA	ICHEC-EC-EARTH	RCA4
CNR-RCA	CNRM-CM5	RCA4
MPI-RCA	MPI-ESM-LR	RCA4

2.2. Generalized Extreme Value (GEV) Distribution

Flood quantiles are calculated by fitting a Generalized Extreme Value (GEV) distribution to the annual maximum series (Equation (1)). The GEV distribution with the L-Moment method has been selected following the national recommendations in the region where the catchments are located [23,24]. In addition, the GEV distribution is applied widely in earth system sciences and hydrology to study extremes of several natural phenomena, including rainfall, floods, wind speeds and wave heights [25].

The cumulative distribution function $F(x)$ of the GEV distribution is expressed with the following equation:

$$F(x) = \exp\left[-\left\{1 - k \frac{(x - u)}{\alpha}\right\}^{1/k}\right], \quad (1)$$

where u is the location parameter, α is the scale parameter, and k is the shape parameter.

The GEV distribution function allows us to obtain the peak flow and precipitation quantiles for high return periods needed for the study.

2.3. HBV Model and Calibration

The hydrological response in the four catchments has been simulated with the continuous HBV rainfall-runoff model. Specifically, the HVB-light-GUI 4.0.0.7 version has been used.

The HBV model is a semi-distributed model, dividing a given catchment into elevation and vegetation zones, as well as into sub-catchments. The model supplies simulations of catchment discharge on a daily time step. The model consists of three routines: Snow, soil and groundwater. Each routine provides a flow time series depending on a set of parameters. The snow accumulation and snowmelt are computed by a degree-day method in the snow routine. In the soil routine, groundwater recharge and actual evapotranspiration are simulated as functions of actual water storage. In the groundwater routine, runoff is computed as a function of water storage. Finally, in the routing routine, a triangular weighting function is used to simulate the routing of the runoff until the catchment outlet [26]. Parameters values related to the soil routine have been estimated initially using land-use maps supplied by the CORINE land cover.

The model parameters have been calibrated using Monte Carlo simulations and GAP optimization. Both tools are integrated into the HBV software.

Model parameters have been calibrated using the coefficient of efficiency (Reff) goodness-of-fit function that is integrated into the HBV software. ‘Reff’ compares the prediction supplied by the HBV

model with the simplest possible prediction, which is a constant value equal to the mean value of observations over the entire period (Equation (2)):

$$R_{eff} = 1 - \frac{\sum (Q_{sim}(t) - Q_{obs}(t))^2}{\sum (Q_{obs}(t) - \overline{Q_{obs}})^2}, \quad (2)$$

where $Q_{sim}(t)$ is the simulated discharge at time step t , $Q_{obs}(t)$ is the observed discharge at time step t and $\overline{Q_{obs}}$ is the mean value of the observed discharges.

A sensitivity analysis with 1,000,000 Monte Carlo simulations was conducted to identify the most important parameters in the four catchments. Maximum storage capacity in the soil (FC), maximum flow from upper to lower box (PERC), upper storage character coefficient 0 (K0) and upper storage recession coefficient 1 (K1) were found to be the characteri that had the most influence on the results. FC, PERC, K0 and K1 are associated with soil infiltration processes that are characterized with three boxes [27]. As expected, the snow routine is not important in the case studies.

Flood quantiles have been estimated by fitting a GEV distribution to the annual maximum series of streamflow observed and simulated by the HBV model. Flood quantiles obtained by simulation have been compared with flood quantiles obtained from observed data, for a set of return periods (Figure 2). An iteration process has been used, prioritizing the similarity in the simulation of high return period quantiles, as the results of the study will be applied to dam design.

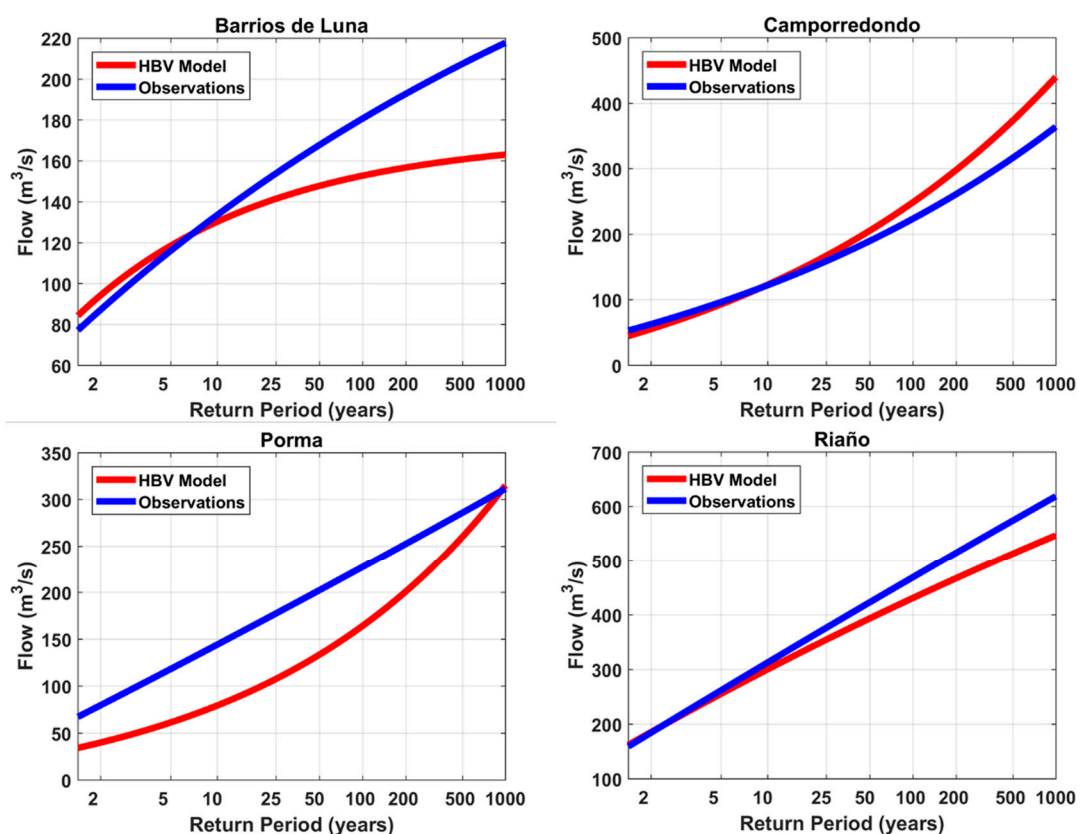


Figure 2. Comparison between HBV results and observations in the control period.

2.4. Bias Correction

Statistics of precipitation and temperature projections supplied by climate models in the control period do not usually fit exactly those of observations in the same period. Such errors may affect simulated flow results in the future period. Bias correction methods try to improve the fitting of climate model simulations to observations in the control period, in order to enhance the reliability

of climate model results in the future period. First, temperature and precipitation series have been corrected separately with a set of methodologies. Second, temperature and precipitation bias correction techniques are combined to identify the best methodology.

2.4.1. Temperature Correction

Temperature projections have been corrected by using simple seasonal bias correction [6]. Mean monthly temperatures are obtained in each climate model in the control period for its comparison with observations in the same period. The difference between climate model simulations and observations is added to the projections in the future period for the two emission scenarios (Equation (3)):

$$T_{i,j,corr} = T_{i,j} + \Delta T_{i,j}, \quad (3)$$

where $T_{i,j}$ is the mean temperature in month j for the climate model i , ΔT is the difference between the mean temperature of the climate model i and the observations in month j , and $T_{i,j,corr}$ is the corrected temperature in month j for the climate model i .

2.4.2. Precipitation Correction

There are several methodologies for correcting bias in precipitation projections [9]. Some methods are simple, consisting of obtaining a rainfall threshold to correct rainfall from 0.1 mm to dry days. Other methods are more complex and require a separate precipitation model. Finally, some methods correct the precipitation based on empirical techniques [28–30].

This study is focused on dam safety. Consequently, extreme events are the variable of interest. The following bias correction techniques for precipitation projections are proposed. First, quantile mapping (QM) linear correction (Equation (4)). Second, QM second-order polynomial correction (Equation (5)) [30,31]. Both methods require to estimate a set of parameters that are adjusted by comparing the observed data with each climate model simulations in the control period. With such parameter values, precipitation projections are corrected in the future periods for the two emission scenarios.

$$P_{i,j,corr} = a \cdot P_{i,j} + b, \quad (4)$$

$$P_{i,j,corr} = c \cdot (P_{i,j})^2 + d \cdot P_{i,j} + e, \quad (5)$$

where $P_{i,j}$ is the raw precipitation supplied by the climate model i in day j , $P_{i,j,corr}$ is the precipitation corrected for the climate model i in day j , and a , b , c , d and e are quantile mapping parameters.

3. Results and Discussion

The best bias correction method has been identified for: (i) Temperature projections, in terms of monthly averages; (ii) extreme precipitation in climate projections, in terms of frequency curves for annual maximum series; and (iii) extreme simulated discharges.

3.1. Bias Correction in Temperature Series

In the four catchments, monthly mean temperatures supplied by climate models are significantly lower than observations (Figure 3), with similar differences in all the months in the range 3–5 °C. While the Porma catchment shows the largest errors, the Barrios de Luna catchment shows the smallest errors.

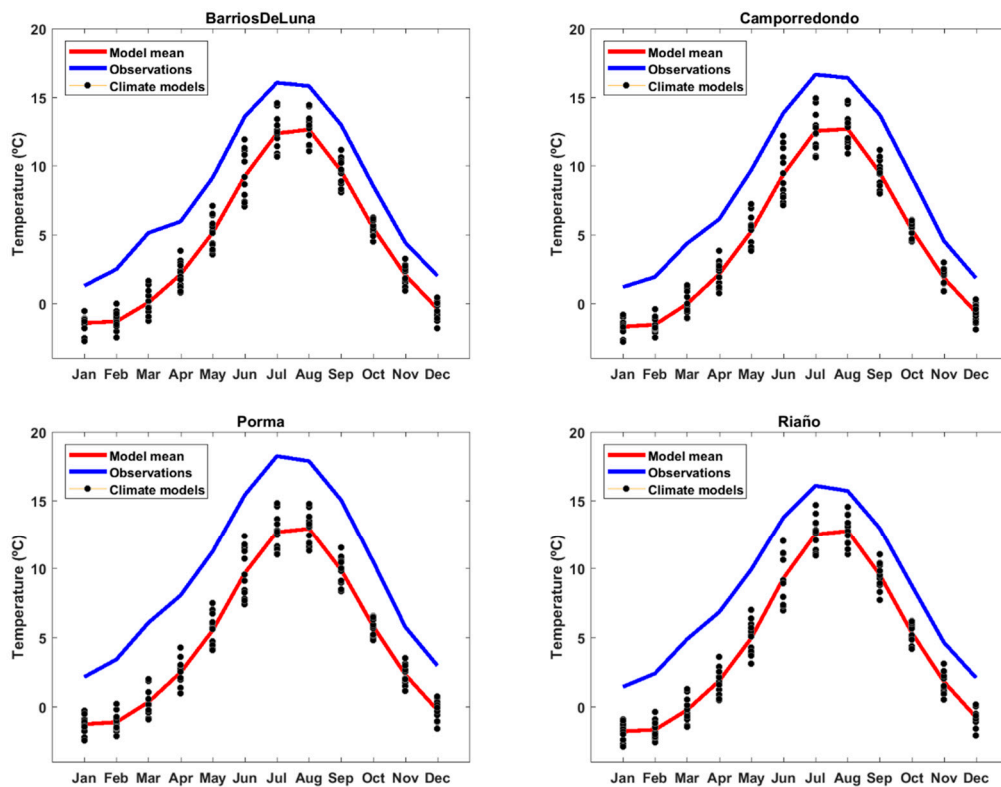


Figure 3. Comparison between monthly mean temperatures supplied by climate models and observations in the control period. Blue lines are observations. Red lines represent the median of the 12 climate models considered.

3.2. Bias Correction in Precipitation Series

Climate models usually supply differing precipitation magnitudes in the control period compared to observations (Figures 4–7). In the Barrios de Luna catchment, climate models supply larger extreme precipitations than observations. However, in the other three catchments, climate models supply lower precipitations.

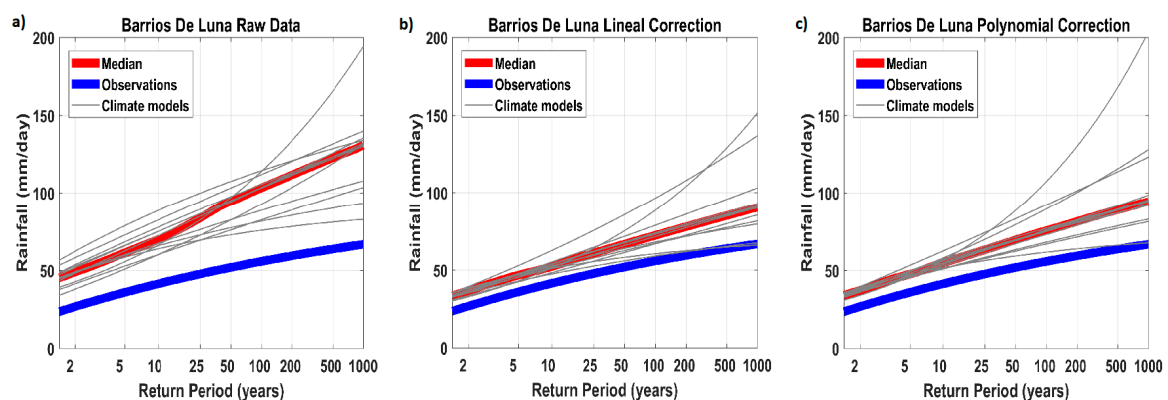


Figure 4. Annual maximum daily precipitation frequency curves in Barrios de Luna catchment. Red lines represent the median of the 12 climate models considered. (a) Raw precipitation supplied by climate models; (b) linear bias correction; (c) polynomial bias correction.

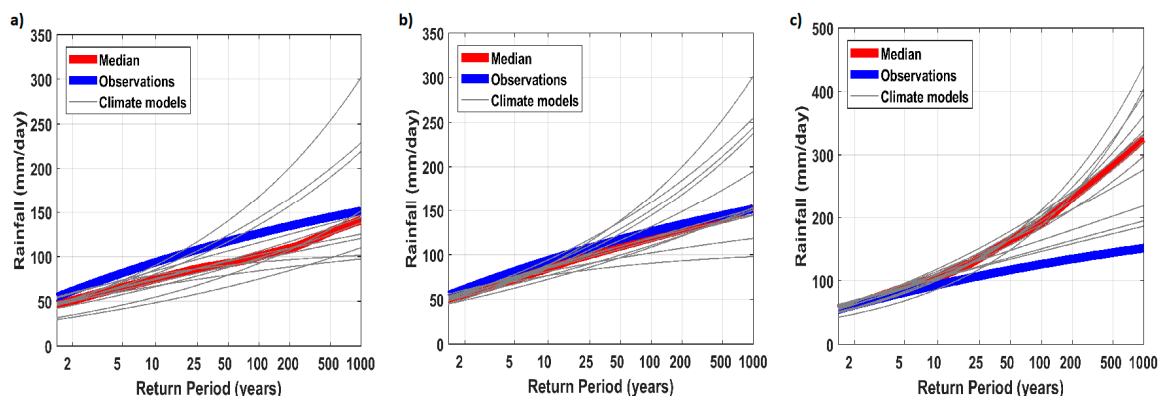


Figure 5. Annual maximum daily precipitation frequency curves in Camporredondo catchment. Blue lines are frequency curves fitted to observations. Red lines represent the median of the 12 climate models considered. (a) Raw precipitation supplied by climate models; (b) linear bias correction; (c) polynomial bias correction.

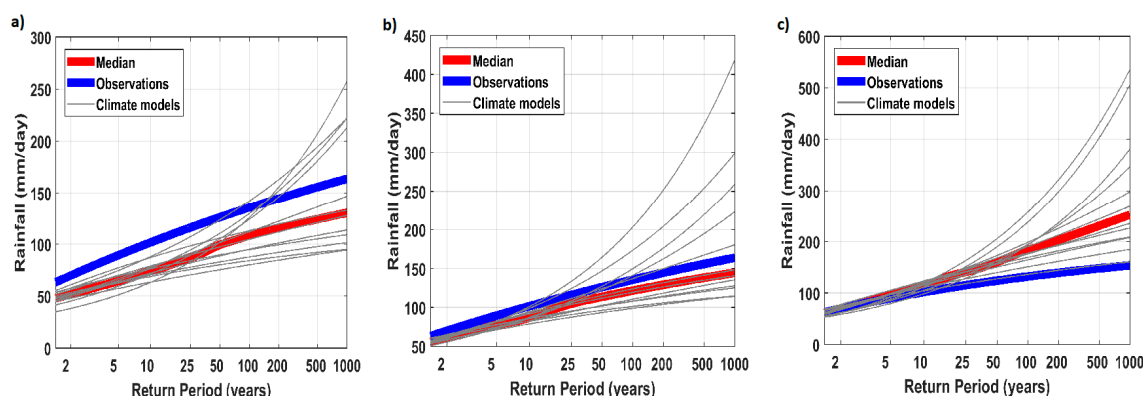


Figure 6. Annual maximum daily precipitation frequency curves in Porma catchment. Red lines represent the median of the 12 climate models considered. (a) Raw precipitation supplied by climate models; (b) linear bias correction; (c) polynomial bias correction.

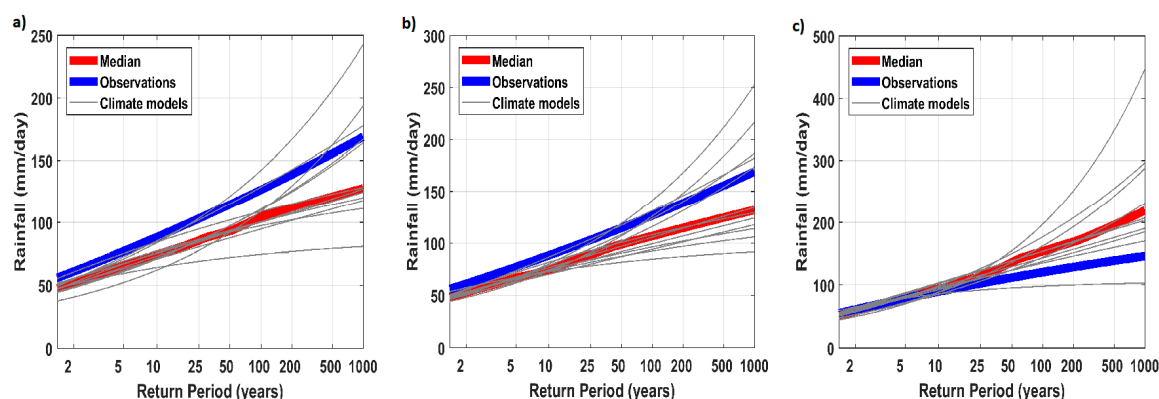


Figure 7. Annual maximum daily precipitation frequency curves in Riaño catchment. Red lines represent the median of the 12 climate models considered. (a) Raw precipitation supplied by climate models; (b) linear bias correction; (c) polynomial bias correction.

As mentioned previously, in the Barrios, the Luna catchment, the observed precipitation data are smaller than climate model projections (Figure 3). Both bias correction techniques reduce errors. However, the QM polynomial correction technique is the best method for this case.

In Camporredondo, Porma and Riaño catchments, frequency curves fitted to observations are slightly larger than the median of the climate model projections (Figures 4–6). The best results are

obtained for the QM linear bias correction technique, as the QM polynomial correction leads to precipitation quantiles larger than observations, especially for high return periods.

Summarizing, bias correction by using both the linear and polynomial techniques reduce errors compared to raw precipitation data in the four catchments, in terms of precipitation frequency curves. The QM linear correction technique is the best bias correction method in three catchments. The QM polynomial correction technique is the best bias correction method in the Barrios de Luna catchment.

3.3. Bias Correction in Terms of Flood Frequency Curves in the Control Period

Simulations of the continuous HBV model have been conducted with a set of combinations of raw and bias corrected temperature and precipitation time series in the control period as input data, in order to compare the bias correction techniques. The best combination of bias correction techniques is identified in terms of the smallest errors in the flood frequency curve estimated with observations. The higher return periods have been considered, due to its importance in dam design.

In the Barrios de Luna catchment, the best fit to the observed data is obtained with raw precipitation and temperature projections with no bias correction (Figure 8). Bias correction in temperature time series leads to similar results, but with larger errors for high return periods, which are used in dam safety. QM precipitation corrections improve the fitting for low return periods, but increase errors significantly for high return periods. Finally, similar results are obtained for combinations of bias correction techniques in both precipitation and temperature series.

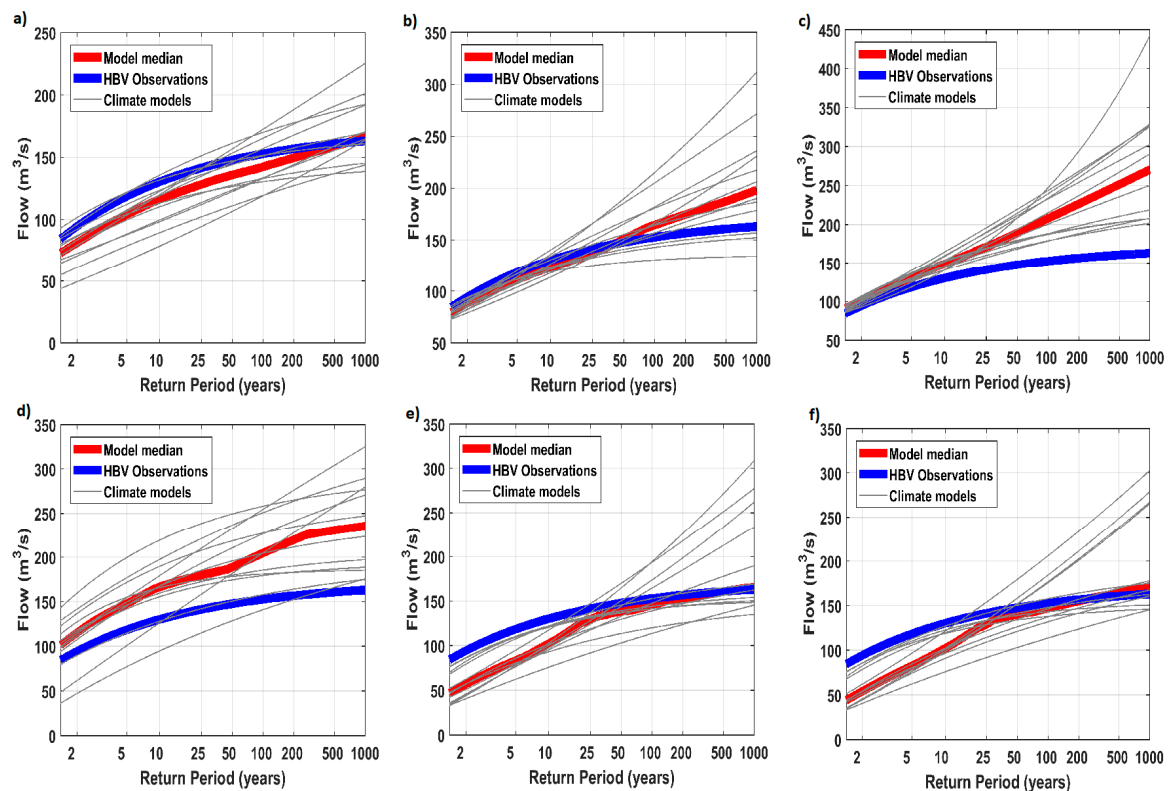


Figure 8. Comparison between flood frequency curves fitted to annual maximum series simulated by the HBV model with observed data and HBV simulations with climate projections in Barrios de Luna catchment, using a set of combinations of bias correction techniques. Red lines represent the median of the 12 climate models considered. (a) Raw data with no bias correction; (b) raw temperature and precipitation with quantile mapping (QM) linear correction; (c) raw temperature and precipitation with QM polynomial correction; (d) raw precipitation and temperature bias corrected; (e) temperature bias corrected and precipitation with QM linear correction; (f) temperature bias corrected and precipitation with QM polynomial correction.

In the Camporredondo catchment, a significant improvement was found by using bias correction techniques in precipitation and temperature data (Figure 9). The polynomial correction in precipitation and temperature series led to the smallest errors.

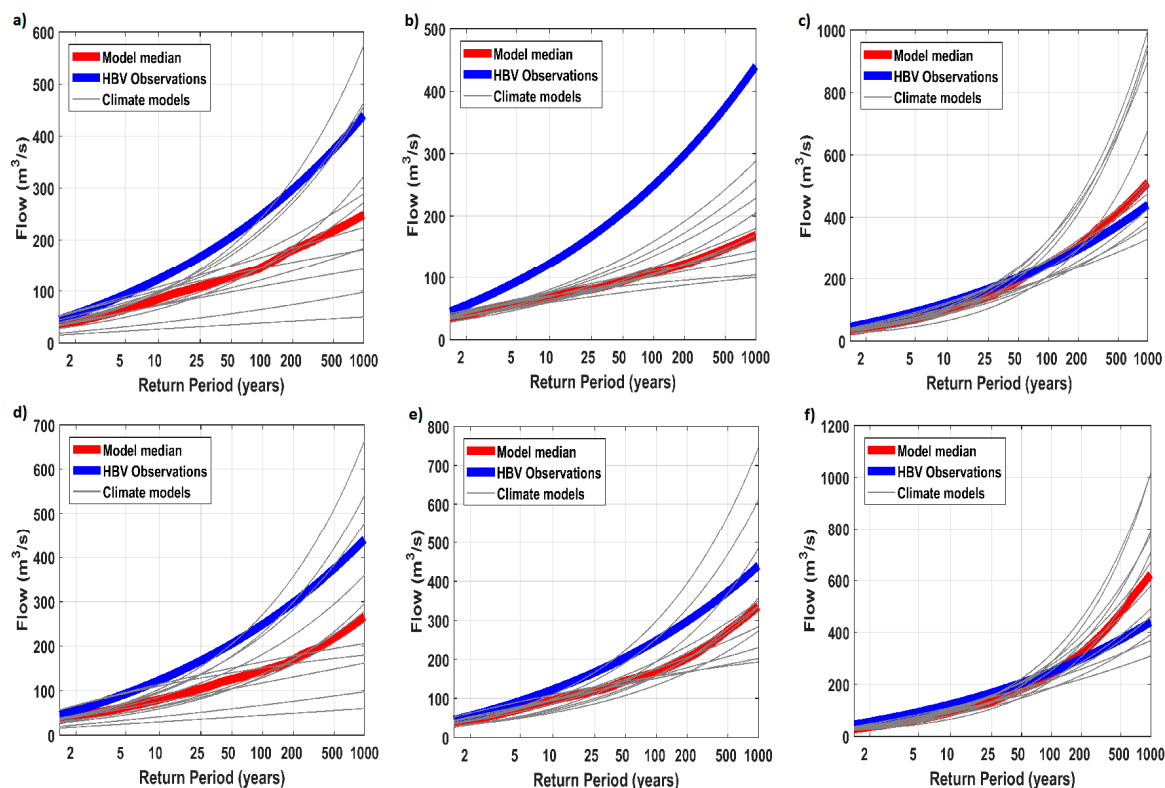


Figure 9. Comparison between flood frequency curves fitted to annual maximum series simulated by the HBV model with observed data and HBV simulations with climate projections in Camporredondo catchment, using a set of combinations of bias correction techniques. Red lines represent the median of the 12 climate models considered. (a) Raw data with no bias correction; (b) raw temperature and precipitation with QM linear correction; (c) raw temperature and precipitation with QM polynomial correction; (d) raw precipitation and temperature bias corrected; (e) temperature bias corrected and precipitation with QM linear correction; (f) temperature bias corrected and precipitation with QM polynomial correction.

The Porma catchment shows larger errors, as the observed data are significantly larger than simulations provided by the HBV model (Figure 10). However, the smallest errors are obtained for temperature bias corrected and precipitation with QM polynomial correction, mainly for high return periods, where the smallest errors are found.

In the Riaño catchment, the temperature correction leads to small changes in flood frequency curves. In this case, the smallest errors are obtained for precipitation data with QM polynomial correction (Figure 11). The technique that leads to the best fit for high return periods is the QM polynomial correction in precipitation data with the raw temperature time series.

In general, the smallest errors are obtained with the polynomial bias correction technique. More specifically, the methodologies with the smallest absolute error for higher return periods are: Raw temperature and raw precipitation supplied by climate models in Barrios de Luna; QM lineal correction for precipitation and mean monthly temperature correction in Camporredondo; QM polynomial correction for precipitation and mean monthly temperature correction in Porma; and QM polynomial correction for precipitation and raw temperature in Riaño.

Finally, the errors of the selected methods in each catchment are summarized in Table 3. In general, smaller errors are obtained for higher return periods, that are usually used for dam design.

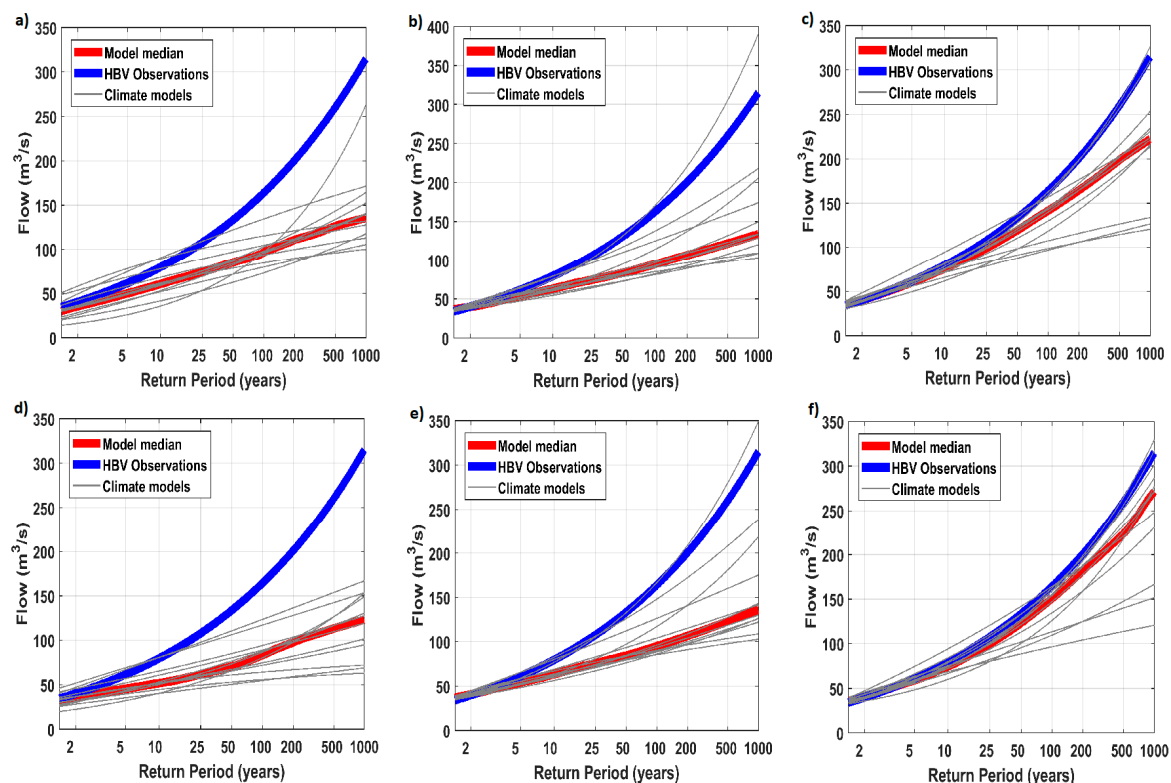


Figure 10. Comparison between flood frequency curves fitted to annual maximum series simulated by the HBV model with observed data and HBV simulations with climate projections in Porma catchment, using a set of combinations of bias correction techniques. Red lines represent the median of the 12 climate models considered. (a) Raw data with no bias correction; (b) raw temperature and precipitation with QM linear correction; (c) raw temperature and precipitation with QM polynomial correction; (d) raw precipitation and temperature bias corrected; (e) temperature bias corrected and precipitation with QM linear correction; (f) temperature bias corrected and precipitation with QM polynomial correction.

3.4. Expected Changes in Flood Frequency Curves in the Future Period

Precipitation and temperature projections in the future period (2011–2095) have been corrected with the best bias correction technique identified in each catchment in the previous step. Such corrected precipitation and temperature time series are used as input data in the HVB model. Annual maximum series of streamflow series simulated by the HBV model is extracted, and flood frequency curves are estimated by using a GEV distribution function. Delta changes in peak flow quantiles expected in the future are obtained by comparing the flood frequency curves in the future and control periods (Figure 12).

In the Barrios de Luna catchment, significant differing results are found between RCP 4.5 and RCP 8.5. In RCP 4.5, flood quantiles are expected to be larger in the two first periods in the future (2011–2040 and 2041–2070), mainly for high return periods, though a decrease in all return periods is expected in the last period (2071–2100). For RCP 8.5, large increases in flood quantiles are expected for the period 2071–2100, though a slight increase and decrease are expected for the periods 2011–2040 and 2041–2070, respectively.

In the Camporredondo catchment, a generalized decrease in flood quantiles is expected in the future periods for both emission scenarios. In the RCP 4.5 scenario, the largest decrease is expected in the period 2071–2100, mainly for high return periods. In addition, minor changes are expected in the period 2041–2070. In the RCP 8.5, the largest decrease in flood quantiles is expected in the period 2041–2070.

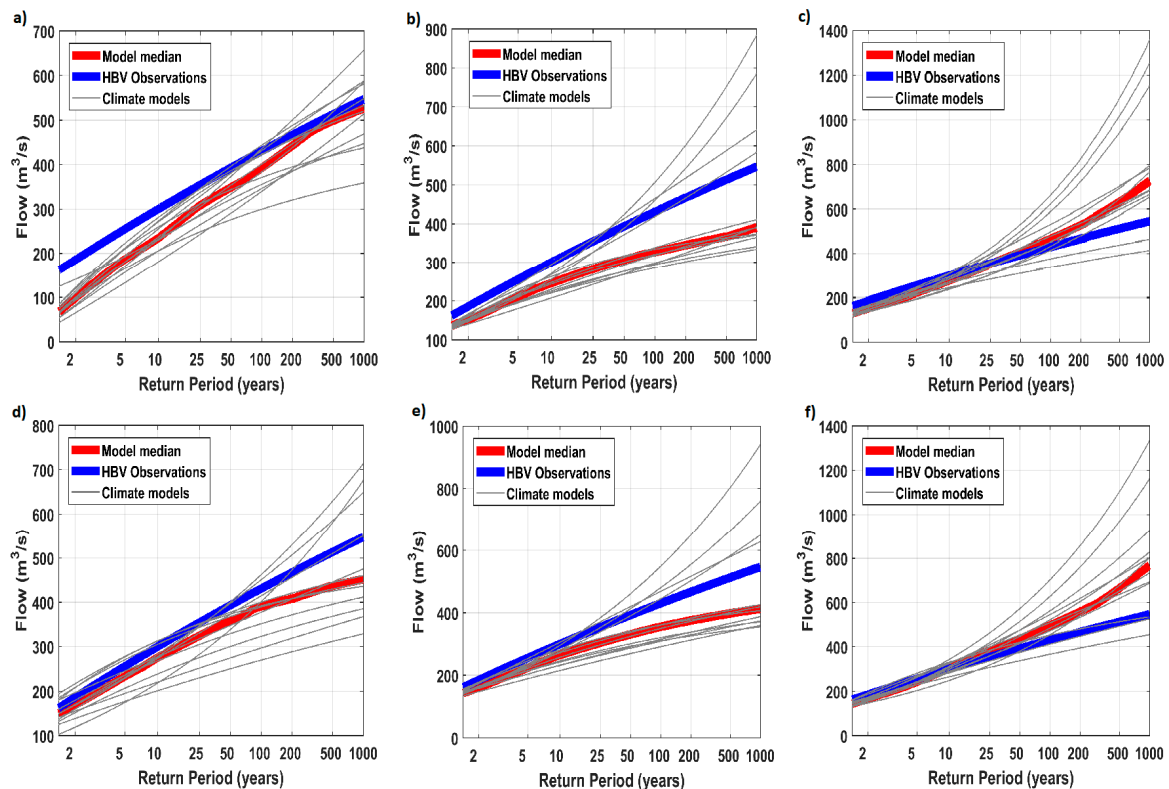


Figure 11. Comparison between flood frequency curves fitted to annual maximum series simulated by the HBV model with observed data and HBV simulations with climate projections in Riaño catchment, using a set of combinations of bias correction techniques. Red lines represent the median of the 12 climate models considered. (a) Raw data with no bias correction; (b) raw temperature and precipitation with QM linear correction; (c) raw temperature and precipitation with QM polynomial correction; (d) raw precipitation and temperature bias corrected; (e) temperature bias corrected and precipitation with QM linear correction; (f) temperature bias corrected and precipitation with QM polynomial correction.

Table 3. Absolute and relative errors of HBV simulations of peak flow quantiles in the control period for the best bias correction method identified in each catchment.

Barrios de Luna									
Tr (Years)	2	5	10	25	50	100	200	500	1000
Absolute error (m ³ /s)	44.72	38.04	28.65	11.08	−6.21	−27.15	−51.96	−91.19	−126.16
Relative error (%)	55.36	32.03	19.43	5.88	−2.79	−10.45	−17.27	−25.22	−30.55
Camporredondo									
Tr (years)	2	5	10	25	50	100	200	500	1000
Absolute error (m ³ /s)	−11.19	−18.35	−23.79	−30.92	−35.89	−39.89	−42.12	−40.41	−33.48
Relative error (%)	−20.28	−20.98	−20.99	−20.33	−19.29	−17.73	−15.63	−11.93	−8.36
Porma									
Tr (years)	2	5	10	25	50	100	200	500	1000
Absolute error (m ³ /s)	−29.58	−43.56	−49.06	−51.09	−48.51	−41.95	−30.85	−7.93	16.85
Relative error (%)	−41.71	−42.17	−39.72	−34.56	−29.41	−23.14	−15.67	−3.67	−7.31
Riaño									
Tr (years)	2	5	10	25	50	100	200	500	1000
Absolute error (m ³ /s)	45.45	31.64	20.30	3.76	−9.78	−23.88	−38.07	−55.80	−67.19
Relative error (%)	42.60	16.76	8.03	1.08	−2.29	−4.62	−6.16	−7.22	−7.41

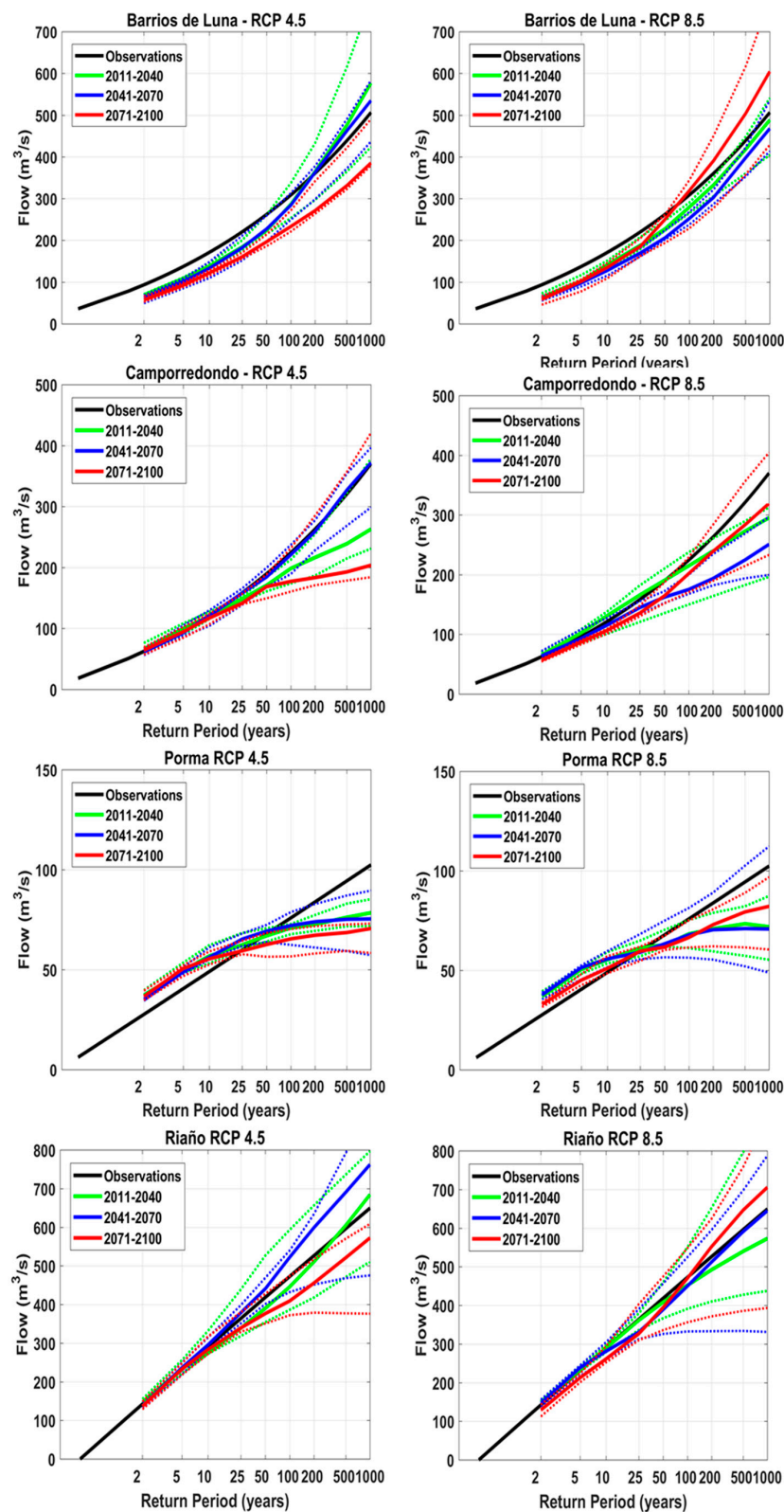


Figure 12. Expected flood frequency curves in the future periods (2011–2040, 2041–2070 and 2071–2100) with the best bias correction techniques identified in the previous section. The dotted lines show the Q_{33} and Q_{67} percentiles for each period. The first column shows the results for RCP 4.5 and the second column for RCP 8.5. The first row shows results for the Barrios de Luna catchment, the second for Camporredondo, the third for Porma and the fourth for Riaño.

In the Porma catchment, similar results are found for all periods and emission scenarios. Flood quantiles will decrease for high return periods, though they will be slightly higher for return periods smaller than 25 years.

Finally, in the Riaño catchment, the results are similar to the Barrios de Luna catchment. In the RCP 4.5, flood quantiles will be larger in the period 2041–2070, smaller in the period 2071–2100 and similar to the control period in 2011–2040. In the RCP 8.5, flood quantiles will be larger in the period 2071–2100, smaller in the period 2011–2040 and similar to the control period in 2041–2070.

Summarising, simulations with the HBV model by using precipitation and temperature projections corrected with the best bias correction techniques identified previously show that, in general, flood frequency curves will decrease in the future, though increases can be seen in some cases.

4. Conclusions

The results of this study confirm the need for bias correction in temperature and precipitation projections to improve their fitting to observations. Mean monthly temperatures supplied by climate models in the control period are significantly lower than observed data. For precipitation projections, annual maximum series are slightly smaller than observations in three of the four catchments considered. In terms of precipitation frequency curves, bias correction reduces errors compared to raw data in the four catchments. The quantile mapping linear correction technique is the best bias correction method in three of the four catchments. It confirms the results of previous studies that found that the quantile mapping technique is the best approach to correct extreme values of precipitation.

A set of combinations of bias correction methods for precipitation and temperature were analyzed, by comparing the outputs of the HBV model with the observations in the control period. Flood frequency curves fitted to simulations and observations were compared. The best bias correction method for precipitation projections, in terms of precipitation frequency curves, differs from the best method in terms of flood frequency curves. It was found that bias correction of precipitation time series is more important than temperature correction, as precipitation has a larger influence on streamflow outputs of the HBV model. This finding agrees with previous studies that highlighted the importance of correcting biases in precipitation projection with advanced techniques, while correcting only mean values in temperature projections. In terms of flood frequency curves, the best bias correction technique for precipitation is the quantile mapping polynomial correction. Both raw temperature projections and bias corrected temperature time series lead to similar results in terms of flood frequency curves.

Simulations with the HBV model in the future period, using temperature and precipitation projections corrected with the best combination of bias correction techniques identified in each catchment, show a general reduction in flood quantiles, smoothing the increases identified in precipitation quantiles. For example, in the control period, when precipitation quantiles are larger than observations, flood quantiles are similar to observations. In general, the period 2071–2095 presents the smallest reductions and, in some cases, the largest increases. This finding agrees with previous studies that stated that floods could decrease in many parts of southern Europe under climate change conditions.

Author Contributions: E.S. wrote the manuscript, conducted the analyses and was the person in charge of the review process. C.G. supplied the climate projection data in the case studies that was processed previously. L.M. coordinated the analyses conducted in the paper and edited the manuscript.

Funding: The authors acknowledge that this study was supported by the project CGL2014-52570-R ‘Impact of climate change on the bivariate flood frequency curve’ of the Spanish Ministry of Economy and Competitiveness.

Acknowledgments: The authors acknowledge the ‘Fundación Carlos González Cruz’. In addition, the authors would like to thank AEMET and the Centre for Hydrographic Studies of CEDEX for providing the data used in this study.

Conflicts of Interest: The authors declare no conflict of interest.

Abbreviations

AEMET	Agencia Española de Meteorología
CORDEX	Coordinated Regional Climate Downscaling Experiment
GAP	Genetic Algorithm and Powell
GCM	General Climate Model
GEV	Generalized extreme value
HBV	Hydrologiska Byråns Vattenbalansavdelning

References

- Intergovernmental Panel on Climate Change (IPCC). *The Physical Science Basis. Contribution of Working Group I to the Fourth Assessment Report of the Intergovernmental Panel on Climate Change*; Cambridge University Press: Cambridge, UK, 2007; Volume 996.
- McCarthy, J.J.; Canziani, O.F.; Leary, N.A.; Dokken, D.J.; White, K.S. (Eds.) *Climate Change 2001: Impacts, Adaptation, and Vulnerability: Contribution of Working Group II to the Third Assessment Report of the Intergovernmental Panel on Climate Change*; Cambridge University Press: Cambridge, UK, 2001; Volume 2.
- Baratti, E.; Montanari, A.; Castellarin, A.; Salinas, J.L.; Viglione, A.; Bezzi, A. Estimating the flood frequency distribution at seasonal and annual time scales. *Hydrol. Earth Syst. Sci.* **2012**, *16*, 4651–4660. [[CrossRef](#)]
- Kundzewicz, Z.W.; Krysanova, V.; Dankers, R.; Hirabayashi, Y.; Kanae, S.; Hattermann, F.F.; Huang, S.; Milly, P.C.D.; Stoffel, M.; Matczak, P.; et al. Differences in flood hazard projections in Europe—their causes and consequences for decision making. *Hydrol. Sci. J.* **2017**, *62*, 1–14. [[CrossRef](#)]
- Eden, J.M.; Widmann, M.; Maraun, D.; Vrac, M. Comparison of GCM-and RCM-simulated precipitation following stochastic postprocessing. *J. Geophys. Res. Atmos.* **2014**, *119*, 11040–11053. [[CrossRef](#)]
- Bergström, S.; Carlsson, B.; Gardelin, M.; Lindström, G.; Pettersson, A.; Rummukainen, M. Climate change impacts on runoff in Sweden assessments by global climate models, dynamical downscaling and hydrological modelling. *Clim. Res.* **2001**, *16*, 101–112. [[CrossRef](#)]
- Christensen, J.H.; Boberg, F.; Christensen, O.B.; Lucas-Picher, P. On the need for bias correction of regional climate change projections of temperature and precipitation. *Geophys. Res. Lett.* **2008**, *35*, L20709. [[CrossRef](#)]
- Teutschbein, C.; Seibert, J. Regional climate models for hydrological impact studies at the catchment scale: A review of recent modeling strategies. *Geogr. Compass* **2010**, *4*, 834–860. [[CrossRef](#)]
- Schmidli, J.; Frei, C.; Vidale, P.L. Downscaling from GCM precipitation: A benchmark for dynamical and statistical downscaling methods. *Int. J. Climatol.* **2006**, *26*, 679–689. [[CrossRef](#)]
- Leander, R.; Buishand, T.A.; van den Hurk, B.J.J.M.; de Wit, M.J.M. Estimated changes in flood quantiles of the river Meuse from resampling of regional climate model output. *J. Hydrol.* **2008**, *351*, 331–343. [[CrossRef](#)]
- Déqué, M.; Rowell, D.P.; Lüthi, D.; Giorgi, F.; Christensen, J.H.; Rockel, B.; Jacob, D.; Kjellström, E.; de Castro, M.; van den Hurk, B. An intercomparison of regional climate simulations for Europe: Assessing uncertainties in model projections. *Clim. Chang.* **2007**, *81*, 53–70. [[CrossRef](#)]
- Teutschbein, C.; Seibert, J. Bias correction of regional climate model simulations for hydrological climate-change impact studies: Review and evaluation of different methods. *J. Hydrol.* **2012**, *456*, 12–29. [[CrossRef](#)]
- De Lara, E.P. *Método de Regionalización de Precipitación Basado en Análogos*; Agencia Estatal de Meteorología: Madrid, Spain, 2008.
- De Lara, E.P. *Método de Regionalización de Temperatura Basado en Análogos*; Agencia Estatal de Meteorología: Madrid, Spain, 2008.
- Jacob, D.; Petersen, J.; Eggert, B.; Alias, A.; Christensen, O.B.; Bouwer, L.M.; Braun, A.; Colette, A.; Déqué, M.; Georgopoulou, E. EURO-CORDEX: New high-resolution climate change projections for European impact research. *Reg. Environ. Chang.* **2014**, *14*, 563–578. [[CrossRef](#)]
- Borén, R.; Ribalaygua, J.; Balairón, L. *Método Analógico de Simulación de Escenarios Climáticos a Escala Comarcal*; Informe Técnico: Madrid, Spain, 1997.
- Garijo, C.; Mediero, L.; Garrote, L. Usefulness of AEMET generated climate projections for climate change impact studies on floods at national-scale (Spain). *Ing. Agua* **2018**, *22*, 153–166. [[CrossRef](#)]
- Garijo, C.; Mediero, L. Assessment of changes in annual maximum precipitations in the Iberian Peninsula under climate change. *Water* **2019**. submitted.

19. Garijo, C.; Mediero, L. Quantification of the expected changes in annual maximum daily precipitation quantiles under climate change in the Iberian Peninsula. *Proceedings* **2019**, *7*, 23. [[CrossRef](#)]
20. Hakala, K.; Addor, N.; Seibert, J. Hydrological modeling to evaluate climate model simulations and their bias correction. *J. Hydrometeorol.* **2018**, *19*, 1321–1337. [[CrossRef](#)]
21. Fang, G.; Yang, J.; Chen, Y.N.; Zammit, C. Comparing bias correction methods in downscaling meteorological variables for a hydrologic impact study in an arid area in China. *Hydrol. Earth Syst. Sci.* **2015**, *19*, 2547–2559. [[CrossRef](#)]
22. Garijo, C.; Mediero, L. Influence of climate change on flood magnitude and seasonality in the Arga River catchment in Spain. *Acta Geophys.* **2018**, *66*, 769–790. [[CrossRef](#)]
23. Martins, E.S.; Stedinger, J.R. Generalized maximum-likelihood generalized extreme-value quantile estimators for hydrologic data. *Water Resour. Res.* **2000**, *36*, 737–744. [[CrossRef](#)]
24. Álvarez, A.J.; Mediero, L.; García, C. Review and selection of statistical models to fit maximum annual peak flows distribution function in Spain. *Ing* **2014**, *104*, 5–31.
25. Hosking, J.R.M.; Wallis, J.R.; Wood, E.F. Estimation of the generalized extreme-value distribution by the method of probability-weighted moments. *Technometrics* **1985**, *27*, 251–261. [[CrossRef](#)]
26. Seibert, J.; Vis, M. Teaching hydrological modeling with a user-friendly catchment-runoff-model software package. *Hydrol. Earth Syst. Sci.* **2012**, *16*, 3315–3325. [[CrossRef](#)]
27. Durman, C.F.; Gregory, J.M.; Hassell, D.C.; Jones, R.G.; Murphy, J.M. A comparison of extreme European daily precipitation simulated by a global and a regional climate model for present and future climates. *Q. J. R. Meteorol. Soc.* **2001**, *127*, 1005–1015. [[CrossRef](#)]
28. Horton, P.; Schaefli, B.; Mezghani, A.; Hingray, B.; Musy, A. Assessment of climate-change impacts on alpine discharge regimes with climate model uncertainty. *Hydrol. Process. Int. J.* **2006**, *20*, 2091–2109. [[CrossRef](#)]
29. Leander, R.; Buishand, T.A. Resampling of regional climate model output for the simulation of extreme river flows. *J. Hydrol.* **2007**, *332*, 487–496. [[CrossRef](#)]
30. Ines, A.V.; Hansen, J.W. Bias correction of daily GCM rainfall for crop simulation studies. *Agric. For. Meteorol.* **2006**, *138*, 44–53. [[CrossRef](#)]
31. Mehrotra, R.; Sharma, A. A multivariate quantile-matching bias correction approach with auto-and cross-dependence across multiple time scales: Implications for downscaling. *J. Clim.* **2016**, *29*, 3519–3539. [[CrossRef](#)]



© 2019 by the authors. Licensee MDPI, Basel, Switzerland. This article is an open access article distributed under the terms and conditions of the Creative Commons Attribution (CC BY) license (<http://creativecommons.org/licenses/by/4.0/>).